Published in final edited form as:

ACS Appl Bio Mater. 2019 October 21; 2(10): 4667–4674. doi:10.1021/acsabm.9b00747.

Synthesis of Ultrasmall Synthetic Melanin Nanoparticles by UV Irradiation in Acidic and Neutral Conditions

Jeanne E. Lemaster[†], **Ananthakrishnan Soundaram Jeevarathinam**[†], **Ajay Kumar**[†], **Bhargavi Chandrasekar**[†], **Fang Chen**[†,§], **Jesse V. Jokerst**[*,†,‡,§]

[†]Department of NanoEngineering, University of California San Diego, 9500 Gilman Drive, La Jolla, California 92093, United States

[‡]Materials Science and Engineering Program, University of California San Diego, 9500 Gilman Drive, La Jolla, California 92093, United States

[§]Department of Radiology, University of California San Diego, 9500 Gilman Drive, La Jolla, California 92093, United States

Abstract

Synthetic melanin nanoparticles have value in metal chelation, photoprotection, and biocompatibility. Applications of these materials have been reported in optics, biomedicine, and electronics. However, precise size control has remained relatively difficult—especially for materials below 1000 nm. In this paper we describe the synthesis of ultrasmall synthetic nanoparticles with size of 9.4–31.4 nm in weakly acidic and neutral conditions via UV-irradiation. Size control of these particles was possible by varying the pH from 6.4–10.0. We then used UV–vis, FTIR, and nuclear magnetic resonance to investigate the mechanism of UV-induced polymerization. The data show that reactive oxygen species from UV irradiation oxidizes intermediates of the reaction and accelerates the formation of these synthetic melanin structures.

Graphical Abstract

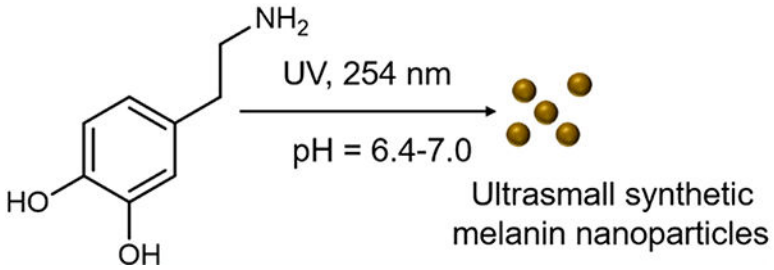

[*]**Corresponding Author:** jjokerst@ucsd.edu.

Author Contributions

The manuscript was written through contributions of all authors. All authors have given approval to the final version of the manuscript.

Supporting Information

The Supporting Information is available free of charge on the ACS Publications website at DOI: 10.1021/acsabm.9b00747.

Additional absorbance data, effect of UV irradiation time on polymerization, reaction rate kinetics, effect of UV controllable on/off polymerization, and additional FTIR data (PDF)

The authors declare no competing financial interest.

Keywords

synthetic melanin nanoparticles; synthesis; polydopamine; UV irradiation; facile preparation; melanin; mechanism

1. INTRODUCTION

Synthetic melanin nanoparticles (SMNPs) are an important class of biobased synthesized nanomaterials that have been used as multimodal imaging agents,[1,2] photothermal agents,[3,4] drug-delivery systems for chemotherapy,[5] and in the fabrication of stimuli-responsive films.[6] In humans, melanins play a diverse role in biological functions such as coloration,[7] chelation,[8] photoprotection,[9] thermoregulation,[10] and quenching of free radicals.[11] Melanins are present within the skin, eye, brain, and hair in two forms: pheomelanin and eumelanin.[12] Pheomelanin is a reddish-yellow pigment that produces free radicals under UV irradiation,[13] cell lysis in Ehrlich ascites carcinoma, and histamine release from mast cells.[14] Eumelanin is a brownish-black pigment and is a known photoprotector, antioxidant, and serves as a marker of Parkinson's disease and melanoma.[15] Eumelanin is typically considered a heteroge- neous macromolecule of 5,6-dihydroxyindole and the 2-carboxylated form, 5,6-dihydroxyindole-2-carboxylic acid. Pheomelanin is a similar heterogeneous macromolecule but includes sulfur from cysteinyldopa.[16] Melanins are formed in nature through the catalytic oxidation of L-tyrosine with tyrosinase.[17] Interestingly, recent work has focused on using synthetic eumelanins as biocompatible platforms in organic electronics, hybrid materials, and biointerfaces.[18] Similar biological-inspired applications of polydopamine (PDA) structures have shown that thin PDA films can attach to a variety of inorganic and organic materials,[19] be used to improve energy production and storage,[20] be used in photocatalytics via Cd^{2+}-loaded PDA precursors,[21] and formulated as a PDA-based gel sunscreen.[22] Multifunctional PDA nanoparticles for tumor-targeted phototherapy using dual peptide RGD- and beclin 1-modified particles has been suggested for improved cancer therapy.[23]

The synthesis of SMNPs typically involves the reaction of dopamine hydrochloride in bases such as NaOH or tris base and subsequent auto-oxidation.[24–26] One of the challenges in the fabrication of SMNPs is the synthesis of ultrasmall nanoparticles (UMNP) with diameters of <50 nm in acidic or neutral conditions. This limits the application of SMNPs where an alkaline condition is prohibited[27] or size control is critical for bioaccumulation in target tissues.[28] SMNPs from 25 to 120 nm have been formed by the autoxidation of dopamine in sodium hydroxide,[25,26] but this approach required alkaline conditions. Microplasma electrochemistry has been used to synthesize fluorescent polydopamine nanoparticles with a size of 3.1 nm using dopamine hydrochloride;[29] however, this method utilized a low pH of 5 and required high-energy electrochemistry, which is expensive. Amin et. al synthesized polydopamine-based melanin-mimetic nanoparticles with diameters from 25–120 nm using sodium hydroxide base.[25] Ultrasmall melanin nanoparticles with a size of 4.5 ± 0.5 nm have also been synthesized by dissolving pristine melanin granules in 0.1 N NaOH and neutralizing under sonication, but required basic conditions and a top-down approach.[30] Wang et al. added varying ratios of edaravone and 2-phenyl-4, 4, 5, 5-

tetramethylimidazoline-1-oxyl 3-oxide (PTIOȮ) to dopamine hydrochloride and added aqueous ammonia to form nanoparticles with size ranging from 155–452 nm.[31] Chen et. al synthesized nanoparticles chelated with Fe^{2+} and Fe^{3+} using sodium hydroxide and PEG.[32] Ni et. al formed water-soluble chitosan-polydopamine nanoparticles with hydrodynamic diameters of approximately 10 nm using tris base and an electrostatic complexation between chitosan and the polymerized dopamine,[33] requiring the use of a base. Finally, Lie et. al formed fluorescent polydopamine dots from the degradation of polydopamine induced by hydroxyl radicals by dissolving dopamine hydrochloride in sodium hydroxide, heating, and aging for 2 weeks.[34]

Synthetic SMNPs are routinely formed from dopamine under basic conditions in solution.[7,24,26,34,35] This approach produces particles typically in size ranges from 100–500 nm via a base-mediated synthesis. In addition, PDA coatings have been described on a variety of underlying substrates using 3,4 dihydroxy L phenylalanine (DOPA),[36] a precursor of dopamine. Interestingly, UV-initiated polymerization of dopamine hydrochloride was used to form polydopamine coatings in both acidic and basic conditions with rapid synthesis and control over the formation of polydopamine micropatterns.[37]

Inspired by this UV-initiated polymerization of polydopamine films, we used UV-irradiation to form ultrasmall melanin nanoparticles <50 nm with size control determined by pH. We believe this is the first example of UV-initiated polymerization of dopamine at this pH range. The product is ultrasmall synthetic melanin nanoparticles with exquisite size control and diameters from 9.4 to 31.4 nm. Additional advantages of this UV-initiated synthesis method include tunable pH conditions, rapid (2 h) synthesis, and controllable kinetics via UV irradiation dose and wavelength.

2. METHODS

Reagents.

The following materials were acquired and used as received: dopamine hydrochloride (Sigma-Aldrich), tris base (Sigma-Aldrich), *diethylhydroxylamine* (DEHA, Sigma-Aldrich), acetone (Sigma-Aldrich), deuterium oxide (D_2O, Cambridge Isotope Laboratories), Xzero Type 1 reference water (XZero).

Instrumentation.

TEM imaging used a Jeol microscope operating at 200 kV. Micrographs were recorded on a 2 K X2 KGatan CCD camera. Absorbance measurements used a Molecular Devices SpectraMax M5 spectrometer, and the absorbance was read in 10 nm increments from 200 nm −1000 nm. Zeta potential was measured using a Zetasizer-90 (Malvern Instruments). pH measurements utilized a Milwaukee MW 102 pH meter and Hydrion pH paper. UV irradiation utilized an 8-W, 0.2 Amps, 115 V, 60 Hz 3UV-38 UV lamp (UVP, USA) at 254 nm unless otherwise indicated. Multispectral advanced nanoparticle tracking analysis (MANTA) utilized the MANTA Instruments ViewSizer 3000 (USA). The FTIR spectra were collected using a PerkinElmer spectrometer (USA). The samples were scanned from 1500 to 600 cm^{-1} and the data were analyzed by PerkinElmer software. The molecular structure was

studied by ^{1}HNMR utilizing a 300 MHz Bruker NMR spectrometer. The spectra were processed using the Topspin 3 program.

Nanoparticle Syntheses.

UMNPwas prepared from dopamine hydrochloride in a method inspired by the synthesis of polymerized dopamine films.[38] In a typical reaction, 200 μL of dopamine hydrochloride aqueous solution was added to a 96-well plate and constantly stirred. The samples were irradiated under UV (254 nm) for 2 h at a constant distance of 3 cm unless otherwise noted. The SMNPs were centrifuged and washed with deionized water three times. The photopolymerized fractions were isolated by filtration through a centrifuge filter with 30 000 Da molecular weight cutoff.

TEM Preparation.

Five microliters of each sample were placed on a Ted Pella 300 mesh Cu TEM 0753-F F/C TEM sample grids. The samples were dried in dark conditions for 1 h prior to imaging.

Size Analysis.

TEM images of at least five fields-of-view of approximately 150 nanoparticles were analyzed using ImageJ software for each synthesis condition. The average size and polydispersity index (PDI) were analyzed for each sample. For multispectral advanced nanoparticle tracking analysis (MANTA) analysis, solutions were prepared with Xzero Type-1 reference water with 30 videos per trial and automated stirring between each video.

Zeta Potential.

UMNP and SMNP was diluted in 500 μL of Millipore water and phosphate buffered saline (PBS) and analyzed with a Zetasizer 90.

pH Readings.

The pH of solutions was measured by analyzing 10 μL of solution with pH paper and/or 1 mL of solution with a pH meter.

Absorbance Readings.

Two hundred microliters of solution were added to wells in 96-well plates. The absorbance was read from 200–1000 nm with a UV–vis spectrometer and plotted using GraphPad Prism Software.

NMR Preparation.

Glassware was washed thrice with acetone and D_2O to remove contaminants. One milliliter of samples (1 mg/mL) was added to 10 mL of D_2O and analyzed in the NMR.

3. RESULTS AND DISCUSSION

The polymerization schematic of dopamine to form synthetic melanin nanoparticles in aqueous solutions with and without UV irradiation is shown in Figure 1. We noted

significant changes in the product as a function of the reaction conditions including pH and UV stimulus suggesting that ultrasmall synthetic melanin nanoparticles could be formed as a function of pH and UV irradiation. The amount of absorbance measured at λ = 280 nm is proportional to the initial concentration of dopamine (Figure S1), indicating that this characteristic peak can be used to estimate the amount of dopamine in solution. The continued presence of this peak at λ = 280 nm after UV irradiation is likely due to either nonreacted dopamine or the presence of small aggregates of dopamine-5,6-dihydroxyindole.[8,39]

From pH 8.0 to 10.0, dopamine polymerizes to form synthetic melanin nanoparticles with or without UV due to the deprotonation of the amine group.[40] At pH 6.4–7.0, dopamine polymerizes under UV irradiation at wavelength of 254 nm; samples without UV mostly remain as the dopamine monomer. Using DOPA as a precursor, Kim et. al suggested that above a pH of 7.0, a deprotonation of the amine site accelerates the intramolecular cyclization to 5,6-dihydroxyin-dole-2-carboxylic acid;[40] a similar effect may be occurring to deprotonate the amine in our experiments with dopamine. Oxidizing the catechol to benzoquinone and the intra- and intermolecular addition of the catechol amines also requires the deprotonation of the amine group.[40,41] UV irradiation is known to generate reactive oxygen species (ROS), which acts as an accelerant in the oxidation steps.[37]

Size Control.

We synthesized synthetic melanin nanoparticles with controllable size ranges from 9.40 to 200 nm by varying the pH of the solution (Figure 2A–E). The average size of the nanoparticles from pH 6.4–10.0 is quantified in Figure 2F. The difference in size is likely due to the difference in deprotonation of the amine group and oxidation steps under UV irradiation.[40] From pH 6.0 to 7.0 with UV irradiation, ROS acts as the accelerant in the oxidation steps[37] to oxidize the catechol to benzoquinone and initialize polymerization. At pH > 7.0, the amine site is deprotonated which accelerates the intramolecular cyclization.[40] Previous studies using a base-mediated approach in synthesis showed that the size of nanoparticles decreases with an increase in pH when pH > 8.0,[43,44] consistent with our findings that the size decreases from pH 9.0 to 10.0. Oxidizing the catechol to benzoquinone and the intra- and intermolecular addition of the catechol amines also requires the deprotonation of the amine group.[40,41] Size control is important for biodistribution of injected particles for vascular targeting, and the enhanced permeability and retention effect (EPR) has can facilitate nanoparticle accumulation with diameters less than 500 nm in tumors.[45] Nanoparticles with diameters <20 nm have been shown to cross tight endothelial junctions, and gold nanoparticles with a diameter of 10 nm were shown to have the widest biodistribution to the blood, liver, spleen, kidney, testis, thymus, heart, lung, and brain compared to larger particles when injected intravenously in rats.[28,45] Dopamine was the only peak observed in the absorbance spectrum in all samples prior to UV irradiation (Figure 2G) with a characteristic peak at 280 nm.[46] After UV irradiation (254 nm), the absorbance spectrum broadened among all samples from a peak at λ = 280 nm to an increase in absorbance 400 nm −1000 nm. This change in absorbance spectrum is a characteristic indication of the formation of melanins[15,47] as the broad absorption band in conjugated systems is caused by the oxidative-polymerization of dihydroxyindole (DHI) and

dihydroxyindole-2-carboxylic acid (DHICA).[40] The careful correlation between TEM and absorption spectroscopy shown here suggested that the width of the absorbance peak directly reports on the extent of dopamine polymerization, and thus subsequent studies primarily utilized absorbance data rather than TEM.

Reaction Time.

The polymerization reaction is also dependent on time; dopamine (5 mg/mL) polymerized after 2 h of UV irradiation (Supplementary Figure S2A), and polymerization increased as UV irradiation time increased. Liu et. al showed synthetic melanin nanoparticle synthesis with a 70 nm size and a 24 h reaction time.[48] Cho and Kim formed synthetic melanin nanoparticles with size range of 80–490 nm using a 3 h reaction time with a hydroxide-ion mediated synthesis.[49] Dopamine (5 mg/mL) in dark conditions at a pH of 6.4 (Figure S2B) does not polymerize even after 8 h, indicating that UV irradiation is necessary under pH conditions of 6.4 to deprotonate the amine and accelerate the intramolecular cyclization to 5,6-dihydroxyindole-2-carboxylic acid.[40]

SMNP formed at pH 10.0 with UV irradiation for 24 h showed increased polymerization (Figure 3A) versus SMNP formed in basic conditions of pH 10.0 in the dark for 24 h (Figure 3B). This was indicated by the broadening of the absorbance peak from 280 to 400 nm (Figure 3C). Dopamine solution with pH 6.4 in dark conditions for 24 h did not show a change in the characteristic absorbance peak of 280 nm indicating no polymerization and no nanoparticles observed (Figure 3D). UV-irradiated samples of dopamine (5 mg/mL) in pH 6.4 and samples of dopamine (5 mg/mL) in pH 9.0 in dark conditions show a linear, first-order reaction over 2 h (Figure S3). This is consistent with the findings of Herlinger et al., who proposed first-order reaction in the autoxidation of dopamine, where he found the reaction to be first-order in [dopamine].[50] Additionally, the reaction rate increased 4.3 times with UV irradiation versus the dark (Figure S4) showing that UV irradiation is necessary to accelerate the reaction. The change in polymerization rate for 0.1–1 mg/mL initial concentration of dopamine in water is shown in Figure S5; polymerization was observable at 0.2 mg/mL.

Wavelength Effects.

The wavelength of UV irradiation was varied from 254 nm −365 nm and solutions at 254 nm showed the highest amount of polymerization due to higher energy at shorter wavelengths (Figure 3E). At a wavelength of 254 nm, the energy is approximately 7.83×10^{-19} J = 4.89 eV and the energy is approximately 366 nm = 5.43×10^{-19} J = 3.39 eV at a wavelength of 365 nm.[51] It is likely that the higher energy at 254 nm is required to deprotonate the amine and initiate the further oxidation steps.

FTIR Characterization.

The FTIR spectrum was compared between SMNP and UMNP in aqueous solution (Figure 3F). The characteristic peak at 3324 cm^{-1} indicates the presence of hydroxyl groups and the characteristic peak at 1636 cm^{-1} indicates the presence of N–H vibrations.[24] Changing the pH from 6.4 to 10.0 did not greatly affect the FTIR spectra, suggesting that the core composition did not change significantly (Figure S6).

NMR Characterization.

The molecular structure of the UMNP formed during the reaction was studied by ^{1}H NMR spectrum. For this experiment, dopamine monomer and SMNP prepared by base-catalyzed polymerization were used as positive and negative controls. Dopamine hydrochloride dissolved in D_2O yielded two triplets at 2.77 and 3.13 δ (Figure 4A), corresponding to the aliphatic side chains. The aromatic protons on dopamine hydrochloride appeared as closely grouped peaks between 6.3–6.83 δ. The SMNP showed no interpretable ^{1}H NMR signals owing to low solubility. The UMNP showed three peaks between 4.00 and 3.00 δ (Figure 4B). These peaks included two multiplets with intensity ratios of 1:1 and a low broad multiplet. The absence of any aromatic proton signals in the photopolymerized fraction showed that polymerization has occurred due to UV exposure. The relatively narrow appearance of the NMR peaks in the photopolymerized fractions point to the low molecular weight of the chains. The zeta potential of the SMNP was −18.8 mV in water and −19.1 mV in PBS. The zeta potential of the UMNP was −8.49 mV in water and −5.50 in PBS. The less negative surface charge of the UMNP may be due to less deprotonation of the amine group compared to the SMNP. A previous report found the zeta potential from pH 2.5–9.0 ranged from approximately +20 mV to −40 mV based on pH with an isoelectric point at pH 4.0–4.1.[25] Zeta potentials from synthetic melanin nanoparticles formed with varying ratios of edaravone (a radical scavenger) and PTIO· (stable free radicals) ranged from −39.8 to −24.0 mV at a pH of 9.55.[31] Additionally, a previous report of water-soluble chitosan-polydopamine nanoparticles meaured the zeta-potential to be 48 mV.[33]

Mechanism.

Despite the prevalence of melanin nanoparticle synthesis, the exact formation mechanism remains unclear. Ab initio calculations have suggested that planar oligomers are stacked together via π–π interactions in synthetic melanin synthesis.[52] Hong et al. suggested that the dopamine and 5,6 dihydroxyindole self-assemble forming a physical trimer structure.[39] Zhang et. al showed that singlet oxygen ($^{1}O_2$), superoxide (O_2^{-}), peroxide (O_2^{2-}), as well as hydroxyl radicals ($^{\bullet}OH$) are essential to the polymerization of dopamine.[53] Reactive oxygen species including hydroxyl radicals, superoxide radicals, and singlet oxygen are generated under UV irradiation and have increased chemical activity over molecular oxygen. Previous studies showed that ROS can initiate the polymerization of dopamine, and UV irradiation initiates the formation of ROS.[37]

Our data validates the proposed mechanism for dopamine polymerization via UV irradiation suggested by Du et. al[37] (Figure 5A). Dopamine is oxidized to dopamine quinone followed by an intramolecular Michael addition and deprotonation leading to leuco-dopamine chrome.[37,54] Additional oxidation and rearrangement leads to the formation of indole-quinone, which then rearranges to form 5,6-dihydroxyin-dole.[15,37] Dopamine quinone, leuco-dopamine chrome, and 5,6-dihdroxyindole then copolymerize; this polymerization is similar to the natural synthesis of eumelanin. In nature, eumelanin is synthesized from the orthohydroxyation of tyrosine and catalyzed by tyrosine oxidase to yield L-DOPA.[15] With an oxidant such as oxygen or metal cations, an oxidation yields dopaquinone; a Michael addition followed by oxidation yields 5,6-dihdroxyindole or 5,6-dihydroxyindole-2-carboxylic acid, foundations of eumelanins.[15] In our experiments, degassing the atmosphere

with nitrogen showed reduced UV–vis absorption and less color change, suggesting the formation of fewer nanoparticles. A lack of oxygen slows the kinetics of polymerization underscores the need for oxygen (Figure 5B, inset).

To further elucidate the role that oxygen plays in the polymerization of dopamine, we added the diethylhydroxylamine (DEHA) oxygen scavenger to the dopamine solution to prevent ROS generation while under UV irradiation (Figure 5C). The polymerization of the UV-irradiated samples was decreased when DEHA was added. Basic conditions were used with the addition of Tris base because DEHA is basic in water. The reduction in polymerization as measured by absorbance suggests that the dopamine polymerization is triggered by ROS generated by UV irradiation.

4. CONCLUSION

This study details a synthetic melanin-based contrast agent synthesized under UV irradiation. The most important finding is that the synthetic melanin particles could be synthesized under acidic and neutral conditions to form ultrasmall particles via UV irradiation. UV irradiation produces ROS that initiate the polymerization. Size control of the nanoparticles was possible from 9.40 to 200 nm by varying the pH during synthesis.

Supplementary Material

Refer to Web version on PubMed Central for supplementary material.

Funding

J.E.L. acknowledges funding from the National Institutes of Health (NIH) Institutional National Research Service Award T32 CA153915, Cancer Researchers in Nanotechnology (Zhang). J.V.J. acknowledges funding from the NIH (Grants R00 HL117048 and DP2 HL137187) and infrastructure from Grants S10 OD021821 and S10 OD023555. The electron micrographs were taken in the Cellular and Molecular Medicine Electron microscopy core facility which is supported in part by National Institutes of Health Award S10 OD023527. This work was performed, in part, at the San Diego Nanotechnology Infrastructure of UCSD, a member of the National Nanotechnology Coordinated Infrastructure, which is supported by the National Science Foundation (Grant ECCS-1542148). We also acknowledge internal funding from the UC Cancer Research Coordinating Committee.

REFERENCES

(1). Lemaster JE; Wang Z; Hariri A; Chen F; Hu Z; Huang Y; Barback CV; Cochran R; Gianneschi NC; Jokerst JV Gadolinium Doping Enhances the Photoacoustic Signal of Synthetic Melanin Nanoparticles: A Dual Modality Contrast Agent for Stem Cell Imaging. Chem. Mater 2019, 31 (1), 251–259.

(2). Li Y; Xie Y; Wang Z; Zang N; Carniato F; Huang Y; Andolina CM; Parent LR; Ditri TB; Walter ED; et al. Structure and Function of Iron-Loaded Synthetic Melanin. ACS Nano 2016, 10 (11), 10186–10194. [PubMed: 27802021]

(3). Jiang Q; Luo Z; Men Y; Yang P; Peng H; Guo R; Tian Y; Pang Z; Yang W Red Blood Cell Membrane-Camouflaged Melanin Nanoparticles for Enhanced Photothermal Therapy. Biomaterials 2017, 143, 29–45. [PubMed: 28756194]

(4). Tian Y; Zhao Y; Liu W; Liu Y; Tang Y; Teng Z; Zhang C; Wang S; Lu G Photosensitizer-Loaded Biomimetic Platform for Multimodal Imaging-Guided Synergistic Phototherapy. RSC Adv. 2018, 8 (56), 32200–32210.

(5). Zhang R; Fan Q; Yang M; Cheng K; Lu X; Zhang L; Huang W; Cheng Z Engineering Melanin Nanoparticles as an Efficient Drug–Delivery System for Imaging-Guided Chemotherapy. Adv. Mater 2015, 27 (34), 5063–5069. [PubMed: 26222210]

(6). Xiao M; Li Y; Zhao J; Wang Z; Gao M; Gianneschi NC; Dhinojwala A; Shawkey MD Stimuli-Responsive Structurally Colored Films from Bioinspired Synthetic Melanin Nanoparticles. Chem. Mater 2016, 28 (15), 5516–5521.

(7). Xiao M; Li Y; Allen MC; Deheyn DD; Yue X; Zhao J; Gianneschi NC; Shawkey MD; Dhinojwala A Bio-Inspired Structural Colors Produced Via Self-Assembly of Synthetic Melanin Nanoparticles. ACS Nano 2015, 9 (5), 5454–5460. [PubMed: 25938924]

(8). Riley P Melanin. Int. J. Biochem. Cell Biol 1997, 29 (11), 1235–1239. [PubMed: 9451820]

(9). Ortonne JP Photoprotective Properties of Skin Melanin. Br. J. Dermatol 2002, 146, 7–10.

(10). Watt W Thermoregulation and Photoperiodically Controlled Melanin Variation in Colias Eurytheme.Proc. Natl. Acad. Sci. U. S. A 1969, 63, 767–774. [PubMed: 16591777]

(11). Seagle B-LL; Rezai KA; Gasyna EM; Kobori Y; Rezaei KA; Norris JR Time-Resolved Detection of Melanin Free Radicals Quenching Reactive Oxygen Species. J. Am. Chem. Soc 2005, 127 (32), 11220–11221. [PubMed: 16089432]

(12). Simon JD; Peles DN The Red and the Black. Acc. Chem. Res 2010, 43 (11), 1452–1460. [PubMed: 20734991]

(13). Agin PP; Sayre RM; Chedekel MR Photodegradation of Phaeomelanin: An in Vitro Model. Photochem. Photobiol 1980, 31 (4), 359–362. [PubMed: 7384229]

(14). Thody AJ; Higgins EM; Wakamatsu K; Ito S; Burchill SA; Marks JM Pheomelanin as Well as Eumelanin Is Present in Human Epidermis. J. Invest. Dermatol 1991, 97 (2), 340–344. [PubMed: 2071942]

(15). Ball V; Gracio J; Vila M; Singh MK; Metz-Boutigue M.-H. l. n.; Michel M; Bour J. r. m.; Toniazzo V. r.; Ruch D; Buehler MJ Comparison of Synthetic Dopamine-Eumelanin Formed in the Presence of Oxygen and Cu2+ Cations as Oxidants. Langmuir 2013, 29 (41), 12754–12761. [PubMed: 24015825]

(16). Meredith P; Sarna T The Physical and Chemical Properties of Eumelanin. Pigm. Cell Res 2006, 19 (6), 572–594.

(17). Liu Y; Ai K; Lu L Polydopamine and Its Derivative Materials: Synthesis and Promising Applications in Energy, Environmental, and Biomedical Fields. Chem. Rev 2014, 114 (9), 50575115.

(18). d'Ischia M; Napolitano A; Ball V; Chen C-T; Buehler MJ Polydopamine and Eumelanin: From Structure-Property Relationships to a Unified Tailoring Strategy. Acc. Chem. Res 2014, 47 (12), 3541–3550. [PubMed: 25340503]

(19). Liu M; Zeng G; Wang K; Wan Q; Tao L; Zhang X; Wei Y Recent Developments in Polydopamine: An Emerging Soft Matter for Surface Modification and Biomedical Applications. Nanoscale 2016, 8 (38), 16819–16840. [PubMed: 27704068]

(20). Qu K; Wang Y; Vasileff A; Jiao Y; Chen H; Zheng Y Polydopamine-Inspired Nanomaterials for Energy Conversion and Storage. J. Mater. Chem. A 2018, 6 (44), 21827–21846.

(21). Zou Y; Wang Z; Chen Z; Zhang Q-P; Zhang Q; Tian Y; Ren S; Li Y Synthetic Melanin Hybrid Patchy Nanoparticle Photocatalysts. J. Phys. Chem. C 2019, 123 (9), 5345–5352.

(22). Wang C; Wang D; Dai T; Xu P; Wu P; Zou Y; Yang P; Hu J; Li Y; Cheng Y Skin Pigmentation-Inspired Polydopamine Sunscreens. Adv. Funct. Mater 2018, 28 (33), 1802127.

(23). Zhou Z; Yan Y; Wang L; Zhang Q; Cheng Y Melanin-Like Nanoparticles Decorated with an Autophagy-Inducing Peptide for Efficient Targeted Photothermal Therapy. Biomaterials 2019, 203, 63–72. [PubMed: 30852424]

(24). Ju K-Y; Lee Y; Lee S; Park SB; Lee J-K Bioinspired Polymerization of Dopamine to Generate Melanin-Like Nanoparticles Having an Excellent Free-Radical-Scavenging Property. Biomacromolecules 2011, 12 (3), 625–632. [PubMed: 21319809]

(25). Amin D; Sugnaux C; Lau K; Messersmith P Size Control and Fluorescence Labeling of Polydopamine Melanin-Mimetic Nanoparticles for Intracellular Imaging. Biomimetics 2017, 2 (3), 17. [PubMed: 29360110]

(26). Liopo A; Su R; Oraevsky AA Melanin Nanoparticles as a Novel Contrast Agent for Optoacoustic Tomography. Photoacoustics 2015, 3 (1), 35–43. [PubMed: 25893172]

(27). Chen T-P; Liu T; Su T-L; Liang J Self-Polymerization of Dopamine in Acidic Environments without Oxygen. Langmuir 2017, 33 (23), 5863–5871. [PubMed: 28505456]

(28). De Jong WH; Hagens WI; Krystek P; Burger MC; Sips AJ; Geertsma RE Particle Size-Dependent Organ Distribution of Gold Nanoparticles after Intravenous Administration. Biomaterials 2008, 29 (12), 1912–1919. [PubMed: 18242692]

(29). Wang Z; Xu C; Lu Y; Wei G; Ye G; Sun T; Chen J Microplasma Electrochemistry Controlled Rapid Preparation of Fluorescent Polydopamine Nanoparticles and Their Application in Uranium Detection. Chem. Eng. J 2018, 344, 480–486.

(30). Fan Q; Cheng K; Hu X; Ma X; Zhang R; Yang M; Lu X; Xing L; Huang W; Gambhir SS; Cheng Z Transferring Biomarker into Molecular Probe: Melanin Nanoparticle as a Naturally Active Platform for Multimodality Imaging. J. Am. Chem. Soc 2014, 136 (43), 15185–15194. [PubMed: 25292385]

(31). Wang X; Chen Z; Yang P; Hu J; Wang Z; Li Y Size Control Synthesis of Melanin-Like Polydopamine Nanoparticles by Tuning Radicals. Polym. Chem 2019, 10 (10), 4194–4200.

(32). Chen L; Lin Z; Liu L; Zhang X; Shi W; Ge D; Sun Y Fe2+/Fe3+ Ions Chelated with Ultrasmall Polydopamine Nanoparticles Inducing Ferroptosis for Cancer Therapy. ACS Biomater. Sci. Eng 2019, 5 (9), 4861–4869.

(33). Ni Y; Chen F; Shi L; Tong G; Wang J; Li H; Yu C; Zhou Y Facile Preparation of Water-Soluble and Cytocompatible Small-Sized Chitosan-Polydopamine Nanoparticles. Chin. J. Chem 2017, 35 (6), 931–937.

(34). Lin J-H; Yu C-J; Yang Y-C; Tseng W-L Formation of Fluorescent Polydopamine Dots from Hydroxyl Radical-Induced Degradation of Polydopamine Nanoparticles. Phys. Chem. Chem. Phys 2015, 17 (23), 15124–15130. [PubMed: 25820836]

(35). Xiao M; Hu Z; Wang Z; Li Y; Tormo AD; Le Thomas N; Wang B; Gianneschi NC; Shawkey MD; Dhinojwala A Bioinspired Bright Noniridescent Photonic Melanin Supraballs. Science advances 2017, 3 (9), No. e1701151. [PubMed: 28929137]

(36). Lee H; Dellatore SM; Miller WM; Messersmith PB Mussel-Inspired Surface Chemistry for Multifunctional Coatings. Science 2007, 318 (5849), 426–430. [PubMed: 17947576]

(37). Du X; Li L; Li J; Yang C; Frenkel N; Welle A; Heissler, 5.; Nefedov, A.; Grunze, M.; Levkin, P. A. Uv-Triggered Dopamine Polymerization: Control of Polymerization, Surface Coating, and Photopatterning. Adv. Mater 2014, 26 (47), 8029–8033. [PubMed: 25381870]

(38). Xiao M; Hu Z; Wang Z; Li Y; Tormo AD; Le Thomas N; Wang B; Gianneschi NC; Shawkey MD; Dhinojwala A Bioinspired Bright Noniridescent Photonic Melanin Supraballs. Science Advances 2017, 3 (9), e1701151. [PubMed: 28929137]

(39). Hong S; Na YS; Choi S; Song IT; Kim WY; Lee H Non-Covalent Self-Assembly and Covalent Polymerization Co-Contribute to Polydopamine Formation. Adv. Funct. Mater 2012, 22 (22), 4711–4717.

(40). Kim DJ; Ju K-Y; Lee J-K The Synthetic Melanin Nanoparticles Having an Excellent Binding Capacity of Heavy Metal Ions. Bull. Korean Chem. Soc 2012, 33 (11), 3788–3792.

(41). Afkhami A; Nematollahi D; Khalafi L; Rafiee M Kinetic Study of the Oxidation of Some Catecholamines by Digital Simulation of Cyclic Voltammograms. Int. J. Chem. Kinet 2005, 37 (1), 17–24.

(42). McElfresh C; Harrington T; Vecchio KS Application of a Novel New Multispectral Nanoparticle Tracking Technique. Meas. Sci. Technol 2018, 29 (6), 065002.

(43). Ball V, Polydopamine Nanomaterials: Recent Advances in Synthesis Methods and Applications. Front. Bioeng. Biotechnol 2018, 6,DOI: 10.3389/fbioe.2018.00109 [PubMed: 29484294]

(44). Bridelli MG Self-Assembly of Melanin Studied by Laser Light Scattering. Biophys. Chem 1998, 73 (3), 227–239. [PubMed: 17029729]

(45). Decuzzi P; Godin B; Tanaka T; Lee S-Y; Chiappini C; Liu X; Ferrari M Size and Shape Effects in the Biodistribution of Intravascularly Injected Particles. J. Controlled Release 2010, 141 (3), 320–327.

(46). Wang HY; Sun Y; Tang B Study on Fluorescence Property of Dopamine and Determination of Dopamine by Fluorimetry. Talanta 2002, 57 (5), 899–907. [PubMed: 18968694]

(47). Meredith P; Powell BJ; Riesz J; Nighswander-Rempel SP; Pederson MR; Moore EG Towards Structure-Property-Function Relationships for Eumelanin. Soft Matter 2006, 2 (1), 3744.

(48). Liu Y; Ai K; Liu J; Deng M; He Y; Lu L Dopamine-Melanin Colloidal Nanospheres: An Efficient near-Infrared Photothermal Therapeutic Agent for in Vivo Cancer Therapy. Adv. Mater 2013, 25 (9), 1353–1359. [PubMed: 23280690]

(49). Cho S; Kim S-H Hydroxide Ion-Mediated Synthesis of Monodisperse Dopamine-Melanin Nanospheres. J. Colloid Interface Sci 2015, 458, 87–93. [PubMed: 26210098]

(50). Herlinger E; Jameson RF; Linert W Spontaneous Autoxidation of Dopamine.J. Chem. Soc.j Perkin Trans. 2 1995, No. 2, 259–263.

(51). Raffa RB; Valdez JM; Holland LJ; Schulingkamp RJ Energy-Dependent Uv Light-Induced Disruption of (–) Sulpiride Antagonism of Dopamine. Eur. J. Pharmacol 2000, 406 (3), R11–R12. [PubMed: 11040357]

(52). Chen C-T; Martin-Martinez FJ; Jung GS; Buehler MJ Polydopamine and Eumelanin Molecular Structures Investigated with Ab Initio Calculations. Chemical science 2017, 8 (2), 1631–1641. [PubMed: 28451292]

(53). Zhang C; Ou Y; Lei WX; Wan LS; Ji J; Xu ZK Cuso4/H2o2-Induced Rapid Deposition of Polydopamine Coatings with High Uniformity and Enhanced Stability. Angew. Chem., Int. Ed 2016, 55 (9), 3054–3057.

(54). Salomä ki M; Marttila L; Kivela H; Ouvinen T; Lukkari J Effects of Ph and Oxidants on the First Steps of Polydopamine Formation: A Thermodynamic Approach. J. Phys. Chem. B 2018, 122 (24), 6314–6327. [PubMed: 29787272]

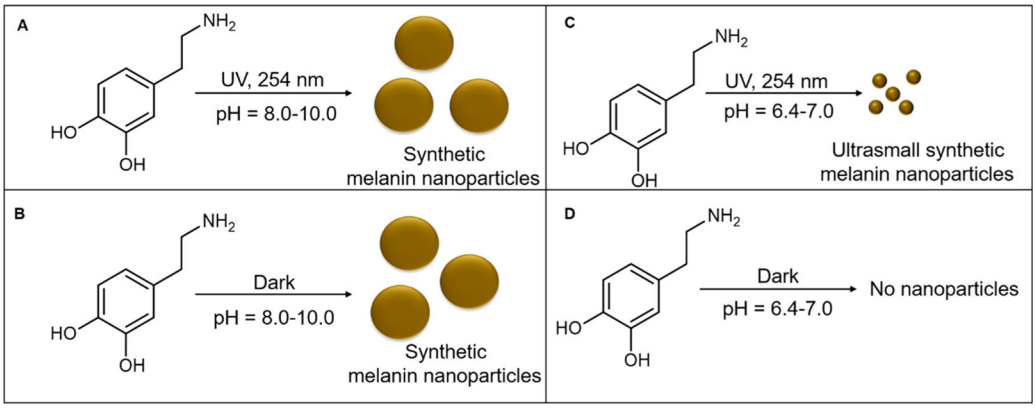

Figure 1.

Synthesis and characterization of ultrasmall synthetic melanin nanoparticles. Ultrasmall synthetic melanin nanoparticles were made by the polymerization of dopamine in aqueous solution with UV irradiation at a wavelength of 254 nm. (A) Dopamine polymerizes under UV in basic conditions at pH = 8.0–10.0 to form synthetic melanin nanoparticles (SMNPs). (B) Dopamine polymerizes in the dark in basic conditions at pH 8.0–10.0 to form synthetic melanin nanoparticles. (C) Dopamine polymerizes under UV in acidic conditions at pH 6.4–7.0 to form ultrasmall synthetic melanin nanoparticles (UMNPs). (D) Dopamine does not polymerize in the dark at pH 6.4–7.0 conditions.

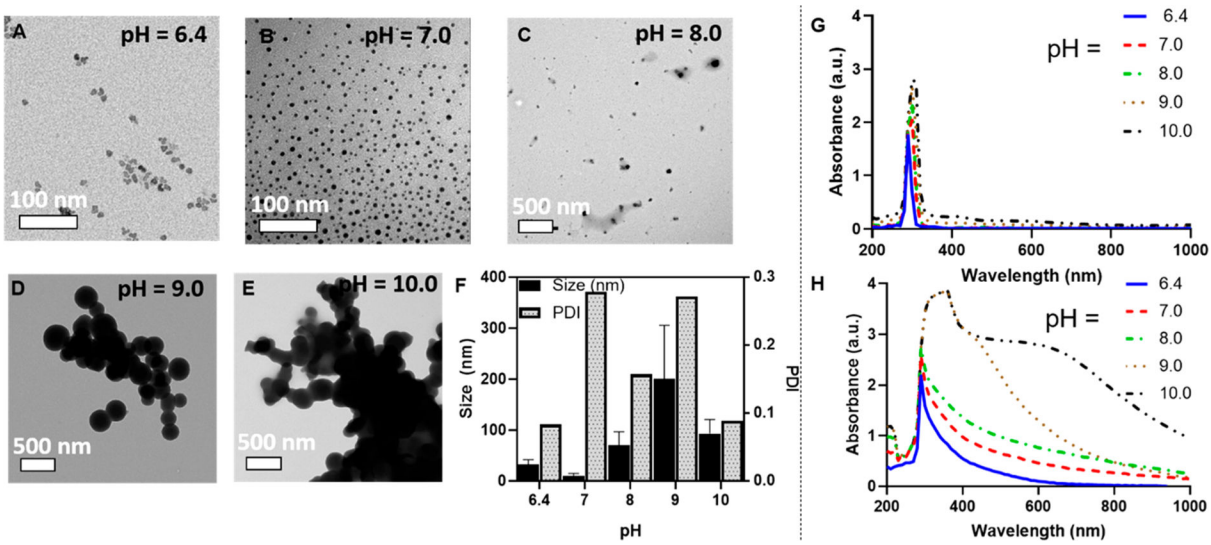

Figure 2.

TEM and absorption spectrum of SMNP and UMNP at initial concentration of 1 mg/mL dopamine. (A) TEM image of UMNP formed at pH 6.4 with 24 h UV irradiation; the average size is 31.4 nm. The size was confirmed with multispectral advanced nanoparticle tracking analysis (MANTA) analysis,[42] indicating a mode size of 34 nm of all particles measured. (B) TEM image of UMNP formed at pH 7.0 with 24 h UV irradiation indicated an average size of 9.40 nm. (C) TEM image of SMNP formed at pH 8.0 with 24 h UV irradiation indicated average size of 69.2 nm. (D) TEM image of SMNP formed at pH 9.0 with 24 h UV irradiation indicated average size of 200 nm. (E) TEM image of SMNP formed at pH 10.0 with 24 h UV irradiation indicated average size of 92.8 nm. (F) Size dependence on pH. The sample with pH 7.0 yielded the smallest spherical UMNP under UV irradiation. (G) Absorbance spectrum based on pH from 6.4 to 10.0 prior to UV irradiation shows the characteristic dopamine peak at 280 nm. (H) Absorbance spectrum based on pH from 6.4 to 10.0 shows a broadening of the characteristic dopamine peak from 280 to 1000 nm, indicating polymerization of UMNP and SMNP.

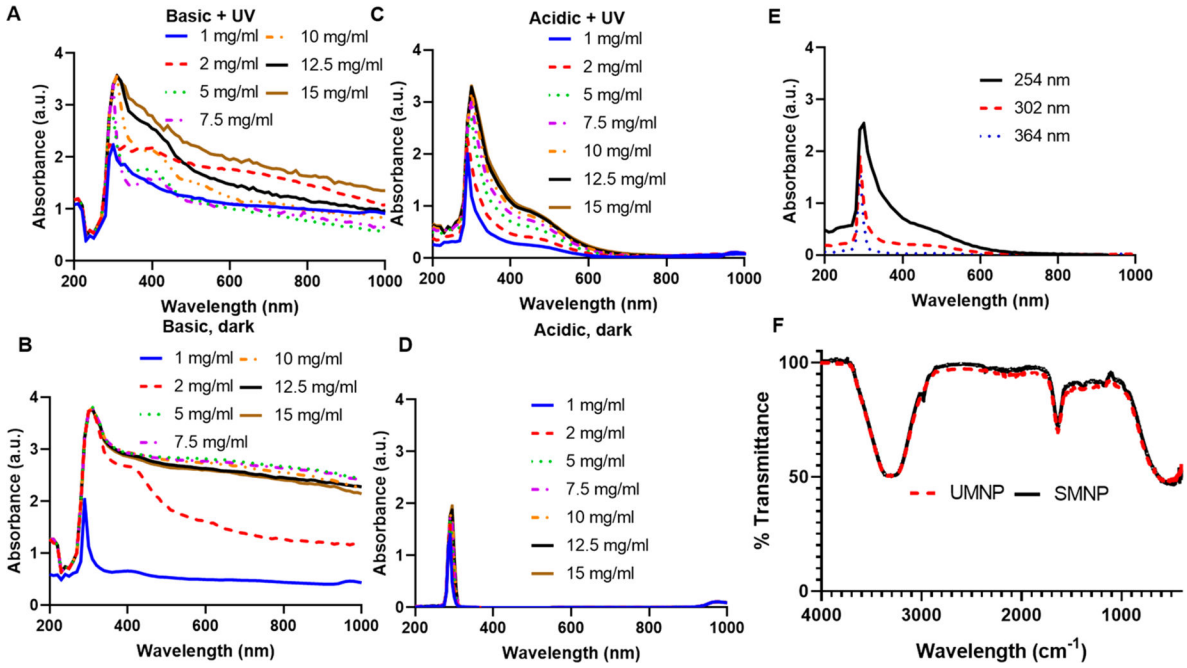

Figure 3.

Characterization of SMNP and UMNP formed in water with UV irradiation at varying concentrations. (A) Basic dopamine solutions with pH 10.0 displayed polymerization with UV irradiation (254 nm) for 24 h and showed a broad peak shift from 290–400 nm at initial concentrations of dopamine of 1–15 mg/mL. (B) Dopamine solutions with pH 10 showed polymerization in the dark after 24 h. (C) Acidic dopamine solutions with pH 6.4 with initial dopamine concentrations from 1 to 15 mg/mL were irradiated with UV light (254 nm) for 24 h to form UMNP. Absorbance increased as concentration of dopamine increased with a red shift in the absorbance spectrum. (D) Acidic dopamine solutions with pH 6.4 in dark conditions for 24 h showed a characteristic dopamine peak at 280 nm and did not show polymerization. (E) UV wavelength of 254 nm irradiated for 24 h causes higher polymerization in dopamine than samples irradiated at 302 and 364 nm for 24 h. Polymerization does not occur when samples are irradiated at 364 nm for 24 h. (F) FTIR spectrum of SMNP (pH 10.0) compared to UMNP (pH 6.4) show similar FTIR spectrum. Characteristic peaks at 3324 and 1636 cm^{-1} indicate the presence of hydroxyl groups and N–H vibrations, respectively.[24]

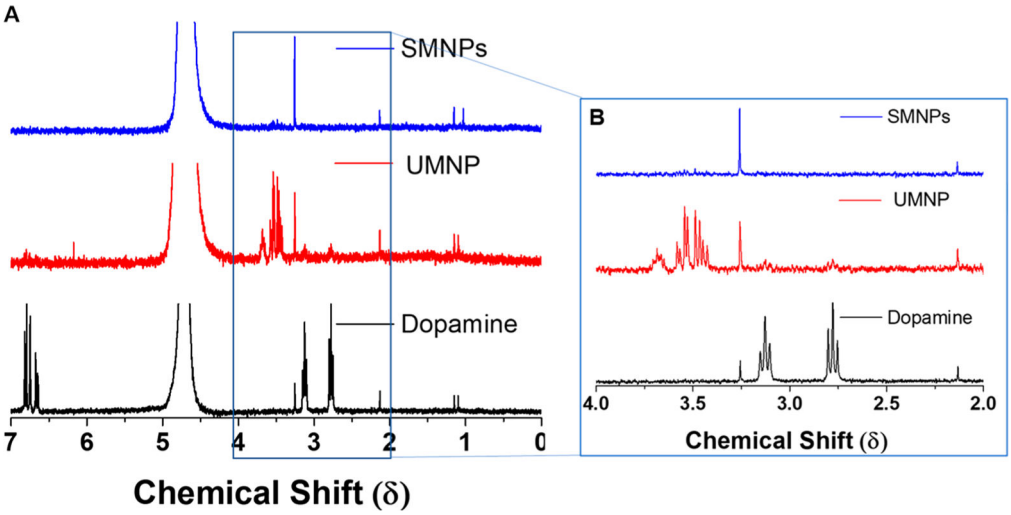

Figure 4.

NMR spectroscopy shows loss of aliphatic side chains in UMNP indicating that polymerization has occurred. (A) Stacked NMR spectrum of SMNPS, UMNP, and dopamine. (B) Dopamine hydrochloride dissolved in D_2O yielded two triplets at 2.77 and 3.13 δ corresponding to the aliphatic side chains.

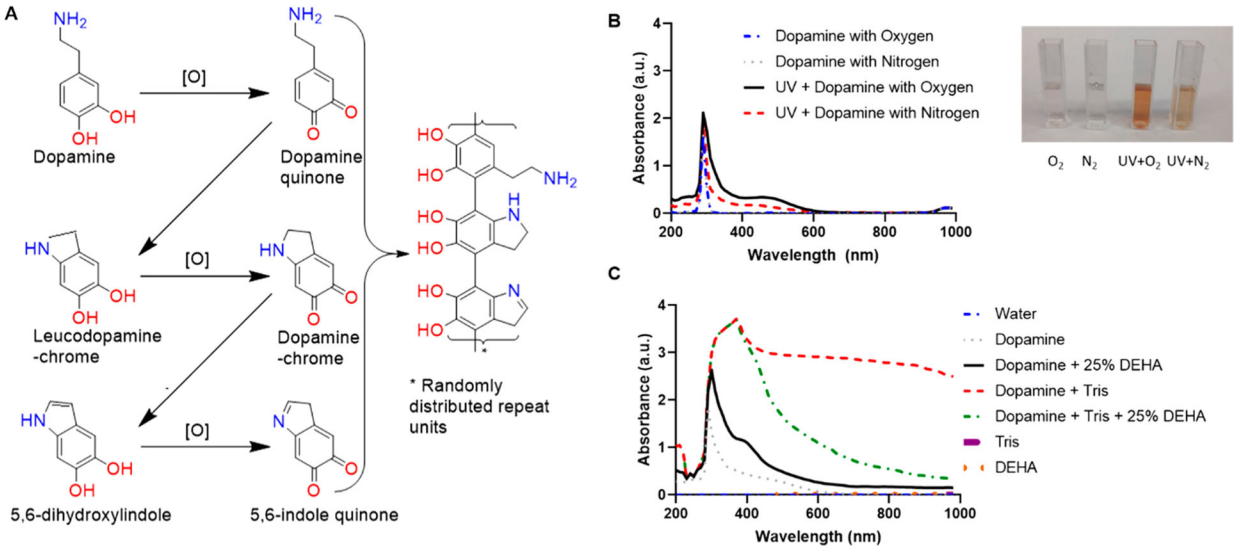

Figure 5.

Mechanism of UV-initiated polymerization. (A) Under the presence of oxygen, dopamine forms dopamine quinone, dopamine-chrome, and 5,6-indole quinone. Adapted with permission from ref 37. Copyright 2014 Wiley. (B) Dopamine under a typical atmosphere (inset, O_2) and a nitrogen degassed atmosphere (inset, N_2) without UV irradiation display a characteristic peak at 280 nm with no polymerization after 24 h. Dopamine irradiated with UV under an oxygenated atmosphere displays polymerization by turning to the characteristic dark brown color (inset, UV + O_2). Dopamine irradiated with UV under a nitrous atmosphere displays little polymerization (inset, UV + N_2). (C) Dopamine under basic conditions (Tris base) shows increased polymerization as indicated by a broad absorption from 280 to 1000 nm when compared to dopamine with tris base and 25% DEHA (oxygen scavenger), indicating that oxygen plays a critical role in the polymerization mechanism.